

Thermal Design And Modelling of a Steam Reformer For Solid Oxide Fuel Cell Fed By Natural Gas

Özer Öğüçlü*, Oğuz Emrah Turgut**[‡], M. Turhan Çoban***

*Ege University, Faculty of Engineering, Department of Chemical Engineering

** Bakırçay University, Faculty of Engineering, Department of Mechanical Engineering

***Ege University, Faculty of Engineering, Department of Mechanical Engineering

(First Author Mail Address, Second Author Mail Address, Third Author Mail Address)

[‡] Corresponding Author; Oğuz Emrah Turgut, Tel: +90 537 729 95 83,

oeturgut@hotmail.com

Received: 12.02.2019 Accepted:25.06.2019

Abstract- In this study, a compact heat exchanger type steam reformer has been modelled for solid oxide fuel cells fed by natural gas. The commercial CFD code COMSOL Multiphysics has been used for modelling the steam reformer. It has been considered that the heat for the endothermic catalytic reactions in the steam reforming processes is gained from the hot exhaust gases of the solid oxide fuel cell. Thus it has been modelled that these hot gases flow through one side of the heat exchanger. In the other side of the heat exchanger, area in which the mixture of steam and methane mixture flows through a catalyst. This area has been modelled as a porous medium because of the catalyst particles. It is shown that hydrogen yield at the exit of the steam reformer and the change of amount of the hydrogen yield are strongly connected with various model parameters.

Keywords COMSOL Multiphysics, Fuel cell, Hydrogen, Natural gas, Steam reforming.

1. Introduction

Fuel cells can be categorized in type of electrochemical machines that produce electrical energy by means of chemical reactions. Fuel cells are named according to electrolyte type they used. These electrolytes are also determined through the type of fuel involving hydrogen or oxygen. These fuel cells also uses natural gas, methanol or coal gases apart from pure hydrogen gas. Fuel cells are noise-free devices that emit water, heat, and very small amount of emission during its process of operation. Fuel cells have some advantages such that they are relatively small devices compared to their counterparts working with high efficiencies and utilizing the low grade disposed waste heat.

Hydrogen is not primary renewable energy source and can not be found in nature with its pure form. Therefore, it is needed to extract energy from secondary energy sources. Thermal and electrochemical methods are proposed as main procedures to produce hydrogen. As a result of the scientific

studies based on this hot spot research area, realizing the manufacturing of low cost hydrogen producing processes and sustaining hydrogen-rich sources will take a great role in forming the future of fuel cell technologies.

This study presents the utilization of a heat exchanger type steam reformer to be used in Solid Oxide Fuel Cell operated with natural gas based on a simulation model developed in COMSOL 3.5a. Model outputs agree well with the experimental data and usage of COMSOL on this design procedure is verified. Outcomes of the experimental investigations was compared with numerical results obtained from simulations. It was seen that simulations are well matched with experimental data. In the context of this study, the amount of energy required for chatalitic reaction in the process of steam reforming is obtained by the waste exhaust gases emitted from a solide oxide fuel cell. On the other side of the fuel cell, an operational region is evident where a catalyst is located and a mixture of methane and steam forming the significant amount of natural gas is passing

through. This area is modelled to be porous due to the presence of the catalyst. Mathematical models developed for multiple gas mixtures are used to obtain the thermophysical properties of gas mixtures flowing through the heat exchanger. The design is made such that there are small tiny particles of catalysts in a region which is modelled as porous media due to the occurrence of catalyst. Variety of properties of a porous media including porosity and permeability are investigated and their corresponding application on a simulated model is maintained. The amount of hydrogen obtained from the fuel cell and its variational changes as a result of varying design parameters are examined by means of a numerical model developed in COMSOL Multiphysics.

2. Hydrogen Energy

The term hydrogen is linguistically composed of “hydro = water” and “genes = birth” and symbolized with H as a first element of the periodic table with an atomic weight of 1. It was invented in the early years of 1500 and its flammability was discovered in 1700s. Hydrogen is the most abundant element in the universe. It is a toxic free element with having no smell and color. Hydrogen which is a main energy source of the universe is also fuel of the heat which is released through the thermonuclear reaction occurred in the sun and other stars. In atmospheric conditions, Hydrogen gas turns into liquid at $-252.77\text{ }^{\circ}\text{C}$ [1].

Amongst the all known type of fuels available, hydrogen has the most amount of energy compared to the others. 1 kg hydrogen contains the same amount of energy available in 2.1 kg natural gas or 2.8 kg petroleum. Hydrogen is 1.33 times more efficient than the petroleum type fuels. Energy system using hydrogen as a primary fuel emits only water or steam to the environment. There is no possibility of producing hazardous chemical product and releasing environment polluting toxic gases such as carbon dioxide and carbon monoxide those increasing the greenhouse effect of the atmosphere during the energy production from hydrogen. Hydrogen gas not only can be produced through different methods but can also be generated by varying energy sources including wave, tide, and biomass which are some kind of derivatives of water and solar energy. Pure hydrogen can not be found in nature, it exists in compound form. Water is the most well known type of its compound. Apart from that, it is generally found attached with organic compounds. Therefore, hydrogen should be dissociated from the compounds in the nature in order to be utilized as an energy source. Its production process is not as easy and profitable as the canned fuels like petroleum. However, its production from the water with the help of solar and tidal energy and its conversion to water after its utilization are the major factors those considerably differ hydrogen from other type of fuels. Hydrogen is a renewable energy source and this intrinsic characteristic makes it available for every option for its production and utilization, different from the underground resources [1].

3. Fuel Cells

Fuel cells are devices that converts chemical energy to electrical energy by means of chemical reactions. Contrary to conventional energy generating cell batteries, fuel cells converts the chemical energy supplied in the process to electrical energy rather than using stored chemical energy. Sustainability of electrical energy can be maintained by continuity of the supplied fuel. Fuel cells have the capability of generating electricity similar to traditional generators. Like all electrochemical systems, fuel cells are comprised of anode and cathode electrodes and electrolytes providing the ion transfer between these two electrodes.

Fuel cell stack are formed by serial connection of many cells. While size of the cell surface area determines the obtainable amount of electrical current, number of cell in the stack designates the operating voltage of the cell. Energy conversion is more efficient compared to that made in thermal cycles as this process is made by virtue of electrochemical cycle that turns chemical energy to electrical energy [1]. Due to the some inherent characteristic advantages such as being noise free applications and emitting zero pollutants when hydrogen is used, utilization of fuel cells in energy production is the most environment-friendly option among the other alternatives. High investment cost values and relatively short service life are two major drawbacks that hamper the utilization of fuel cells in a wide range of application areas.

Fuel cells are categorized into different classifications according to electrolyte type used. Different fuel cell types can be given as follows: proton exchange membrane fuel cell, alkaline fuel cell, phosphoric acid fuel cell, molten carbonate fuel cell, and solid oxide fuel cell.

4. Steam Reformer

Nowadays, there has been developed many systematic procedures to be used for producing hydrogen from a hydrocarbon fuel. Application of these proposed methods depends upon a great deal of system factors such as type of a fuel cell, type of a fuel and so forth. Steam reforming process includes a catalytic reaction between hydrocarbon and steam in order to dissociate fuel bonds and hydrogen bonds of the water molecules. This procedure is a sophisticated and powerful application used for extracting hydrogen from natural gas. Amount of heat required for endothermic catalytic reaction is obtained by direct heating of the tubes containing catalytic beds. A steam reformer with a large surface area is efficient enough for producing hydrogen for fuel cells with power generation of hundreds of MW. However, large surface areas are not suitable for small-scale fuel cells. Having said that, plenty of fuel cell and steam reformer manufacturer benefit the merits large surface areas in manufacturing small scale fuel cells. The most important issue that affects the performance of the fuel cell lies in successful transmission of heat obtained from the burning fuel to steam reformer catalyst [2].

5. Steam reformer model

A steam reformer design is modelled in COMSOL Multiphysics to simulate the mathematical models of energy, momentum, and mass equations. As it was mentioned above sections, steam reformers are used for producing hydrogen to fuel cells. Figure 1 shows the geometric structure of the designated steam reformer discussed in this study. While recycle chemistry takes place in porous catalyst structure, the required heat that will be applied on to accomplish endothermic chemical reactions is supplied from wastes of the hot combustion products coming from the fuel cell.

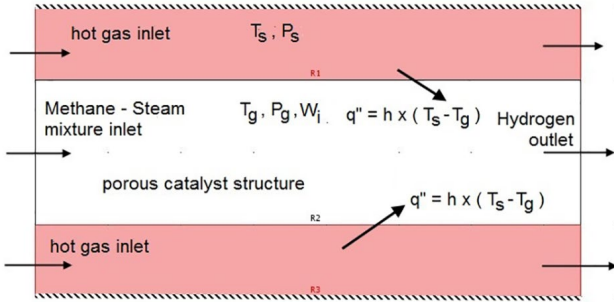
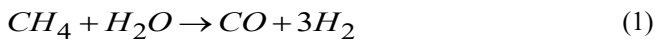
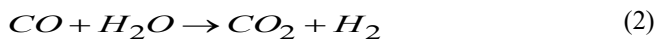


Fig. 1. Figurative description of the steam reformer and related transport mechanisms

Water and steam in the steam reformer react with each other by dint of Ni based catalysts to produce CO, CO₂, and H₂ [3].



$$\Delta H_1 = 206.1 \text{ kJ/mol}$$



$$\Delta H_2 = - 41.15 \text{ kJ/mol}$$



$$\Delta H_3 = 164.9 \text{ kJ/mol}$$

Corresponding reaction rates of the above given equations ($r_i : i = 1,2,3$) are formulated below [3]:

$$r_1 = \frac{1}{(DEN)^2} \frac{k_1}{P_{H_2}^{2.5}} \left(P_{CH_4} P_{H_2O} - \frac{P_{H_2}^3 P_{CO}}{K_1} \right) \quad (4)$$

$$r_2 = \frac{1}{(DEN)^2} \frac{k_2}{P_{H_2}} \left(P_{CO} P_{H_2O} - \frac{P_{H_2} P_{CO_2}}{K_2} \right) \quad (5)$$

$$r_3 = \frac{1}{(DEN)^2} \frac{k_3}{P_{H_2}^2} \left(P_{CH_4} P_{H_2O}^2 - \frac{P_{H_2}^4 P_{CO_2}}{K_3} \right) \quad (6)$$

$$DEN = 1 + K_{CO} P_{CO} + K_{H_2} P_{H_2} + K_{CH_4} P_{CH_4} + \frac{K_{H_2O} P_{H_2O}}{P_{H_2}} \quad (7)$$

Where P_{CH_4} , P_{CO} , P_{H_2O} , and P_{H_2} are partial pressures of the corresponding gases in the control volume; k_i ($i = 1,2,3$) is the rate coefficient of reactions respectively in the form of mol.Pa^{0.5}/kg_{cat}.s and formulated with following equations.

$$k_1 = 8.336 \times 10^{17} \exp(-28879 / T) \quad (8)$$

$$k_2 = 12.19 \exp(-8074.3 / T) \quad (9)$$

$$k_3 = 2.012 \times 10^{17} \exp(-29336 / T) \quad (10)$$

In Eq. 4 to Eq. 7, K_i ($i = 1,2,3$) is the equilibrium constant of reactions and K_j ($j = \{CO, H_2, H_2O, CH_4\}$) are adsorption constants whose respective formulations are defined as below equations.

$$K_1 = 10266.76 \times 10^6 \exp(-26830 / T + 30.11) \quad (11)$$

$$K_2 = \exp(4400 / T - 4.063) \quad (12)$$

$$K_3 = K_1 \cdot K_2 \quad (13)$$

$$K_{CH_4} = 6.65 \times 10^{-9} \exp(4604.28 / T) \quad (14)$$

$$K_{H_2} = 6.12 \times 10^{-14} \exp(9971.13 / T) \quad (15)$$

$$K_{CO} = 8.23 \times 10^{-10} \exp(8497.71 / T) \quad (16)$$

$$K_{H_2O} = 1.77 \times 10^5 \exp(-10666.35 / T) \quad (17)$$

Formation and consumption rates of the above mentioned gases are defined below equations [3]

$$R_{CH_4} = - m_c (\eta_1 r_1 + \eta_3 r_3) \quad (18)$$

$$R_{H_2O} = - m_c (\eta_1 r_1 + \eta_2 r_2 + 2 \eta_3 r_3) \quad (19)$$

$$R_{CO_2} = m_c (\eta_2 r_2 + \eta_3 r_3) \quad (20)$$

$$R_{CO} = m_c (\eta_1 r_1 - \eta_2 r_2) \quad (21)$$

$$R_{H_2} = m_c (3 \eta_1 r_1 + \eta_2 r_2 + 4 \eta_3 r_3) \quad (22)$$

Where m_c is catalyst density and η_i ($i=1,2,3$) are activity coefficients for steam reforming reactions

6. Modelling with COMSOL Multiphysics Simulation Program

Following assumptions are made for fuel cell model simulations

- a- Gas flow across the porous media is modelled through the basics of Darcy law. 59 Kpa pressure drop is considered at the inlet and outlet of steam reformer. All remaining boundaries are considered to be isolated.
- b- Mass balance equations for this simulation are in the form of Maxwell-Stefan diffusion and convection model. Inlet mass ratio for methane is calculated associated with water/carbon ratio. Convection heat flux condition is applied for outlet.

- c- Flowing characteristics of the heating gases in the channels is modelled in terms of weak compressible steady state Navier – Stokes equations. Reference atmospheric pressure is considered. Velocity is taken as constant at inlet and considered zero at the wall and outlet. All viscous stresses are neglected.
- d- Energy transfer in heating channels are defined through the means of conduction and convection. Temperature of heating gases at the inlet is taken 1300 K and it is considered that convection heat transfer is dominant at the exit section of the channels.

Table 1 to Table 5 separately report the thermal and physical conditions of the system parameters.

Table 1 Operating conditions of the steam reformer

Inlet temperature (K)	1300.0
Inlet velocity (m/s)	1.0
Outlet pressure (kPa)	101.0
Convective heat transfer coefficient (W/m²K)	100.0
Mass ratios of the gases	H ₂ O →75% - H ₂ →5.0 % - CO ₂ →10.0% - CO→10.0%
Inlet temperature (K)	1300.0
Inlet velocity (m/s)	1.0
Outlet pressure (kPa)	101.0
Convective heat transfer coefficient (W/m²K)	100.0
Mass ratios of the gases	H ₂ O →75% - H ₂ →5.0 % - CO ₂ →10.0% - CO→10.0%

Table 2 Operational conditions of the methane – steam mixture

Catalyst density (kg_{cat}/m³) [4]	139.0
Catalyst heat conductivity (W/mK) [5]	8.6
Catalyst specific heat (J/kgK)	850.0
Convective heat transfer coefficient (W/m²K)	100.0
Pressure drop (kPa)	10.0
Inlet mass fractions	CH ₄ → 0.228 H ₂ O → 0.769

Table 3 Physical properties of the porous media

<i>Thermal properties</i>	
Body material	AISI 4340 Alloy Steel
Specific heat (J/kgK)	475.0
Density (kg/m³)	7850.0
<i>Constructional properties</i>	
Supporting body (1) length and height (m)	0.15 x 0.10
Catalyst region (1) width and height (m)	0.12 x 0.04
Heating channel (5) width and height (m)	0.02 x 0.02

Table 4 Thermophysical properties of the catalyst

Inlet temperature (K)	750
Inlet pressure (kPa)	111.0
Outlet pressure (kPa)	101.0
Convective heat transfer coefficient (W/m²K)	100.0
Pressure drop (kPa)	10.0
Inlet mass fractions	CH ₄ → 0.228 H ₂ O → 0.769

Table 5 Constructional and thermophysical characteristics of the supporting body of the steam reformer

Porosity [4]	0.47
Permeability (m²)	1x10 ⁻¹⁰
Number of fluidized bed [6]	4

Thermophysical properties of the gas mixtures are determined by obeying the below given assumptions:

- 1- Molar mass of the mixture is computed with both using molar masses and mass fractions of the gasses forming the mixture

$$M_{mix} = \frac{1}{\sum_{i=1}^n \frac{y_{mi}}{M_i}} \quad (23)$$

Where y_{mi} stands for the mass fraction of i^{th} gas in the mixture; M_i is the molar mass of the i^{th} gas in the mixture; and n represents the number of gas in the mixture

- 2- Mole ratio of the components forming the gas mixture is the ratio between partial pressures of the gases and summation of the values of these partial pressures

$$P_i = y_i \cdot P \quad (24)$$

Where y_i is the mol fraction of i^{th} gas in the mixture; P is the working pressure; and P_i is the partial pressure of i^{th} gas in the mixture

- 3- Viscosity of the gas mixture is obtained by using the viscosity of each gas in the mixture through the mathematical model developed by Wilke [7].

$$\mu_{mix} = \sum_{i=1}^n \frac{y_i \mu_i}{\sum_{j=1}^n y_j \phi_{ij}} \quad (25)$$

Where μ_{mix} is the mixture viscosity, n is the number of gas in the mixture y_i is the mol ratio of i^{th} component in the mixture, and μ_i is the viscosity of the i^{th} component in the mixture, and symbol ϕ_{ij} is formulated with the below given equation

$$\phi_{ij} = \frac{\left[1 + \sqrt{\left(\frac{\mu_i}{\mu_j} \right) \left(\frac{M_j}{M_i} \right)^{0.25}} \right]^2}{\sqrt{8 \left(1 + \frac{M_i}{M_j} \right)}} \quad (26)$$

Where M represents the molar mass of the gases in the mixture. Viscosity of the gases are computed by the mathematical model proposed by [8] and [9]

$$\mu_{gas} = 40.785 \frac{F_c \sqrt{MT}}{V_c^{2/3} \Omega_v} \quad (27)$$

Where μ_{gas} symbolizes the viscosity of the gas; T is the gas temperature, V_c is the critical gas volume; and Ω_v is the viscosity collision integral mathematically defined below equation:

$$\Omega_v = A(T^*)^{-B} + C \left[\exp(-D \times T^*) \right] + E \left[\exp(-F \times T^*) \right] \quad (28)$$

Where the model coefficients [10] are $A = 1.16145$, $B = 0.14875$, $C = 0.52487$, $D = 0.77320$, and $E = 2.16178$; and T^* is equated by the following expression

$$T^* = 1.2593 T_r \quad (29)$$

Where T_r is the reduced temperature expressed by

$$T_r = \frac{T}{T_c} \quad (30)$$

Where T_c is the critical temperature. The parameter F_c in Eq.27 is formulated by the following expression

$$F_c = 1 - 0.2756\omega + 0.059035\eta_r^4 + \kappa \quad (31)$$

Where ω is the eccentricity factor; κ is the correction factor for high polarity substances such as alcohols and acids; η_r is dimensionless dipole moment formulated with the following equation

$$\eta_r = 131.3 \frac{\eta}{\sqrt{V_c T_c}} \quad (32)$$

Where η is the dipole moment. These mentioned properties for gases discussed in this study are given in Table 6

Table 6 Critical characteristics of gases discussed in this study

Gases	M (g/mol)	T_c (K)	P_c (bar)	V_c (cm ³ / mol)	ω (-)	η (debye)
CH ₄	16.043	190.4	46.0	99.2	0.011	0.0
H ₂ O	18.015	647.3	221.2	57.1	0.344	1.8
CO ₂	44.010	304.1	73.8	93.9	0.239	0.0

CO	28.101	132.9	35.0	93.2	0.066	0.1
H₂	2.016	33.2	13.0	65.1		

4- Specific heat value of the mixture is summation of the multiplication between specific heats of the gases forming the mixture and their respective mole numbers

$$\bar{c}_{p,mix} = \sum_{i=1}^n y_i \times \bar{c}_{p,i} \quad (33)$$

Where $C_{p,mix}$ is the molar specific heat of the gas mixture; y_i is the mol ratio of the i^{th} component in the mixture; and c_{pi}

is the molar specific heat of the i^{th} component in the mixture. Molar specific heat of the gases in the mixture is calculated by the following equation as a function of operation temperature [13]

$$\bar{c}_p = A + BT + CT^2 + DT^3 + ET^4 \quad (34)$$

Where A to E are gas specific tabular constants reported in Table 7

Table 7 Function coefficients for calculation of the specific heat of the gases

Gases	A	B	C	D	E	F
CH₄	34.942	-3.9970E-2	1.9184E-4	-1.5303E-7	3.9321E-11	50 – 1500 K
H₂O	33.933	-8.4186E-3	2.9906E-5	-1.7825E-5	3.6934E-12	100 – 1500 K
CO₂	27.437	4.2315E-2	-1.9550E-5	3.9968E-9	-2.9872E-13	50 – 5000 K
CO	29.556	-6.5807E-3	2.0130E-5	-1.2227E-8	2.2617E-12	60 – 1500 K
H₂	25.399	-8.4186E-3	2.9906E-5	-1.7825E-8	3.6934E-12	250 – 1500 K

5 – Heat conductivity of the gases forming the gas mixture is calculated by following mathematical model proposed by [11]

$$k_{mix} = \frac{\sum_{i=1}^n y_i k_i}{\sum_{j=1}^n y_j A_{ij}} \quad (35)$$

Where k_{mix} is the thermal conductivity of the mixture; k_i stands for the thermal conductivity of the i^{th} element in the mixture; and A_{ij} is the function proposed by [12]

$$A_{ij} = \frac{1.065 \left[1 + \left(\frac{k_{tri}}{k_{trj}} \right)^{0.5} \left(\frac{M_j}{M_i} \right)^{0.25} \right]^2}{\left[8 \left(1 + M_i / M_j \right) \right]^{0.5}} \quad (36)$$

Where k_{tri}/k_{trj} represents the ratio of monoatomic heat conductivity of the two gases in the mixture and formulated by the below given expression [10]

$$\frac{k_{tri}}{k_{trj}} = \frac{\Gamma_j \left[\exp(0.0464T_{ri}) - \exp(-0.2412T_{ri}) \right]}{\Gamma_i \left[\exp(0.0464T_{rj}) - \exp(-0.2412T_{rj}) \right]} \quad (37)$$

Where $T_r = T / T_c$ is reduced temperature; Γ is the heat conductivity resistance formulated by [10]

$$\Gamma = 210 \left(\frac{T_c M^3}{P_c^4} \right)^{1/6} \quad (38)$$

Heat conductivity of each gas in the mixture is calculated by means of a temperature dependent polynomial function formulated below [10].

$$k = A + BT + CT^2 + DT^3 \quad (39)$$

Table 8 Function coefficients for calculating the thermal conductivity of the gases in the mixture

Gases	A	B	C	D
CH₄	-1.869E-3	8.727E-5	1.179E-7	-3.614E-11
H₂O	7.341E-3	-1.013E-5	1.801E-7	-9.100E-11
CO₂	-7.215E-3	8.015E-5	5.477E-9	-1.053E-11
CO	5.067E-4	9.125E-5	-3.524E-8	8.199E-12
H₂	8.099E-3	6.689E-4	-4.158E-7	1.562E-10

Table 8 reports the constant parameters used in Eq. 39

- 6- Diffusion coefficient of the gas mixture is calculated using the model proposed by Blanc [14] which utilizes the binary gas diffusion coefficients in the form of below given equation

$$D_{i,mix} = \frac{1}{\sum_{\substack{j=1 \\ j \neq i}}^n \frac{y_j}{D_{ij}}} \quad (40)$$

Where $D_{i,mix}$ is the diffusion coefficient of the i^{th} gas in the mixture; $D_{ij(AB)}$ is the binary diffusion coefficient of the gases forming the mixture whose exact formulation is given below [15-17]

$$D_{AB} = \frac{0.00143T^{1.75}}{P \cdot M_{AB}^{0.5} \left[(\Sigma v)_A^{1/3} + (\Sigma v)_B^{1/3} \right]^2} \quad (41)$$

Where P represents the pressure in bar; T is the temperature in Kelvin; $(\Sigma v)_A$ is the atomic diffusion volume of the gas A in the mixture; and M_{AB} is calculated with the following equation

$$M_{AB} = 2 \left[(1/M_A) + (1/M_B) \right]^{-1} \quad (42)$$

Where M_A and M_B are the molar mass of the gas A and gas B in the gas mixture. Atomic diffusion volume values of the gases in the mixture are given in tabular form in Table 9.

Table 9 Diffusion volumes of some atom and molecules

Diffusion volumes of some atoms			
C	15.9	O	6.11
H	2.31	N	4.54
Diffusion volumes of some molecules			
H ₂	6.12	CO ₂	26.9
N ₂	18.5	CO	18.0
O ₂	16.3	H ₂ O	13.1

For instance, diffusion volume of methane gas is calculated by the following equation

$$(\Sigma v)_{CH_4} = 15.9 + 4 \times (2.31) = 25.4 \quad (43)$$

7. Validation of the model

For validation of the presented model, the predictions are compared with experimental data obtained from Hoang’s study [18]. The schematic layout of the equipment system used for Hoang’s experimental study of methane steam reforming is shown in Figure 2.

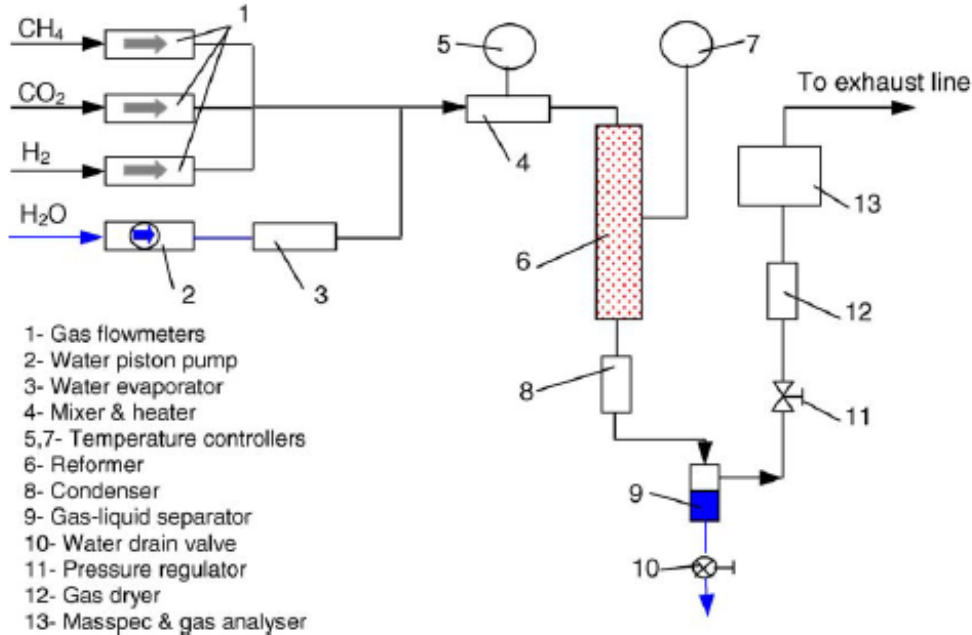


Figure 2. The schematic layout of the equipment system used for Hoang’s experimental study

In this system, gas temperatures and flowrates are controlled according to the set values. The reformer is a stainless steel tube with an inner diameter of 10 mm and total length of 400 mm divided into three zones including preheating zone of 100 mm, reaction zone of 150 mm and cooling zone of 150 mm. The preheating zone is filled with

alumina and heated by a heater, the reaction zone filled with sulfide nickel catalyst and heated by another heater, and the cooling zone filled with inert material. A set of four thermocouples is sliding in a central tube of 2 mm outer diameter to measure and control the preheating and reforming temperatures. The pressure regulator maintains the

backpressure in the system at a stable value. The system operation is controlled by the system controller with a computer interface for monitoring and setting operating parameters. During the steam reforming process, metered water is supplied by the piston pump through the evaporator, mixed with metered methane in the mixer. And then, the mixture of methane and steam is preheated before entering to the reformer containing heated catalyst. The preheating and reforming temperatures are automatically controlled by two temperature controllers. After leaving the reformer, the reformat gas is passed through the condenser, the gas-liquid separator and the gas dryer to remove water content before going to the gas analyzer where its dry composition is determined. The catalyst used in Hoang's study is sulfide nickel catalyst Ni-0309S, supported on gamma alumina. The catalyst is of spherical type and ready for use as supplied. The amount of catalyst loaded in the reaction zone of the reformer is 8.98 g. Once loaded, the catalyst is heated to 773K at 3 K/min in nitrogen and maintained at this temperature for 1 h, and then the catalyst is sustained at the same temperature for 2 h in hydrogen. After that, it is heated

to 1100K at 2 K/min and kept at this temperature for a further hour in hydrogen, and then the temperature is reduced to the required operating temperature. Upon reaching this temperature, the pressure is set to 1.5 bars and the water feed is switched on. The reference conditions for steam reforming operation are set and the experiment is started. The experimental conditions for methane steam reforming in Hoang's study are given in Table 10 and set in a range ensuring the normal and reliable operation of the equipment system and catalyst. The temperature in the reformer evolves from 700 to 1000 K, ensuring high catalyst activity and avoiding reaching a chemical equilibrium. The reformer pressure is regulated at 1.5 bars and the H₂O/CH₄ molar ratio is from 2 to 5.

Comparison of experimental and presented study's mole fractions of CH₄ and H₂O are shown in Figure 3 and comparison of experimental and presented study's mole fractions of H₂, CO₂ and CO are shown in Figure 4.

Table 10 Experimental conditions of the steam reformer in Hoang's study

Porosity	0.35
Tortuosity	1.69
Permeability	5.92x10 ⁻⁹ m ²
Water – Carbon Ratio	3.5
Catalyst	Ni-0309S, supported on gamma alumina

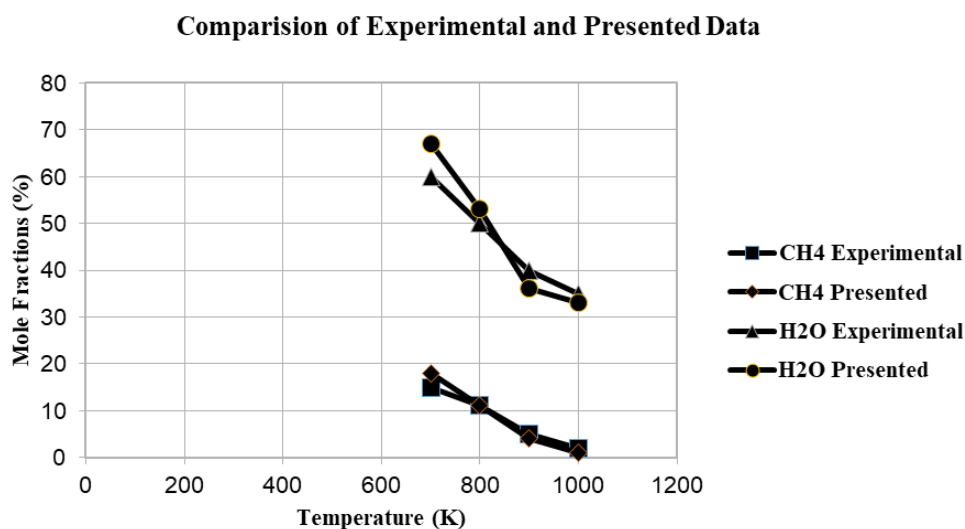


Figure 3. Comparison of experimental and presented study's mole fractions of CH₄ and H₂O

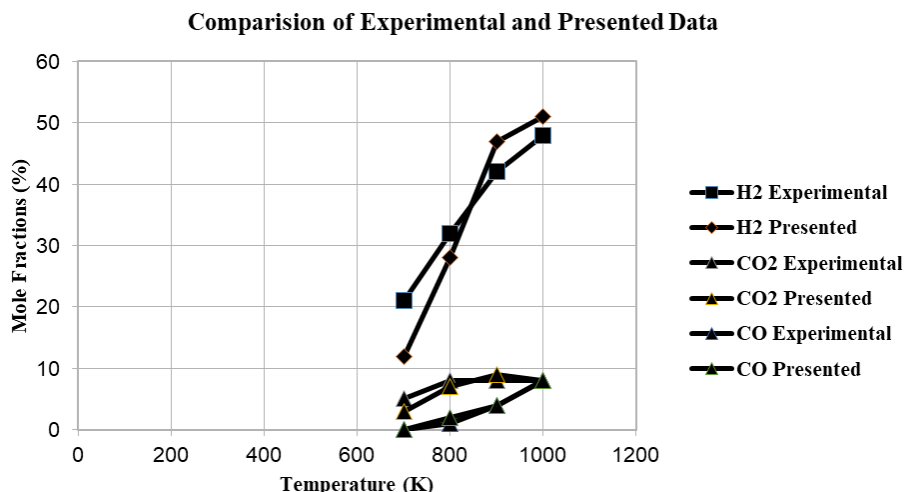


Figure 4. Comparison of experimental and presented study’s mole fractions of H₂, CO₂ and CO

The predictions are in a good agreement with experimental data, so it can be said that the model has a high enough level of confidence for parametric investigation.

8. Results and discussion

Numerical outcomes of the steam reformer simulation developed in COMSOL Multiphysics will be discussed in this section. Variations of temperature distribution and mass fraction of the gases taking place in steam reforming reactions will be explained and visually discussed in terms of figurative descriptions. Figure 5a visualizes the variations of the the mol ratios of the gases those taking place in steam reforming reactions as a function of inlet water/carbon ratios. Steam content in the mixture at the outlet section of steam reformer increases with increasing amount of water/carbon rates, inducing a decrease in methane content in the gas mixture. Mole ratio of hydrogen in the gas mixture decreases to some extent with increasing water/carbon ratio. There is no clear change in carbonmonoxide and carbondioxide rates in the mixture with increasing values of water/carbon ratio. Figure 5b depicts the plot of the effects of water/carbon ratio at the inlet of the steam reformer over the rates of methane conversion ratio. It can be seen that increasing water/carbon ratios leads to an increase in methane conversion ratio. Figure 5c shows the influences of water/carbon ratio at the inlet of the steam reformer on the mass fractions variations of carbonmonoxide and carbondioxide. As it is shown in the figure, increasing water/carbon ratios induces a decline in the mass fraction values of these compounds. Figure 5d plots the effects of the water/carbon ratio at the inlet of the steam reformer over the change of hydrogen mass fraction obtained after the end of steam reforming reactions. Figure 5d shows that increasing water/carbon ratios conduce a decrease in hydrogen mass fraction rates. Figure 6a shows the variational changes of the hydrogen mass fraction during the steam

reforming chemical reactions with varying methane steam mixture inlet pressures at the porous catalyst region. It is clear that the amount of hydrogen in the gas mixture decreases with increasing steam – methane mixture operating pressures. Flow velocities of the gases in porous catalysyt region increase with increasing inlet pressures. However, this increase in flow velocities leads to a decrease in hydrogen formation as the amount of heat transfer required for endothermic reactions does not change during the ongoing reactions. Figure 6b depicts the effects of steam reformer inlet temperatures of steam – methane mixture on the mass fraction of the hydrogen in the mixture. Mass fraction of hydrogen increases to some point with increasing inlet temperatures, nevertheless, a significant decrease trend in hydrogen mass fraction rates is observed after reaching the peak as no enough heat supply is maintained to the heating gases those responsible for sustaining heat transfer for endothermic reactions occurring in steam reformer. Figure 6c shows the influences of the hot gas mixture entering the steam reformer over the amount of the change of the hydrogen mass fraction at the outlet of the steam reformer. It can be observed that hydrogen mass fraction rate increases due to effective provision of heat load obtained from the hot gases that is required for running endothermic reactions taking place in the steam reformer. However, this temperature increase is restricted by the maximum allowable endurance temperature of the steam reformer material. Figure 6d shows the variations of the hydrogen mass fraction in the mixture as a function of activity coefficients for steam reforming reactions. Hydrogen mass fraction in the gas mixture increases with increasing activity coefficient rates. Significance of these activity coefficients should be seriously taken into account as they are strictly associated with catalyst geometry and catalyst arrangement in the steam reformer.

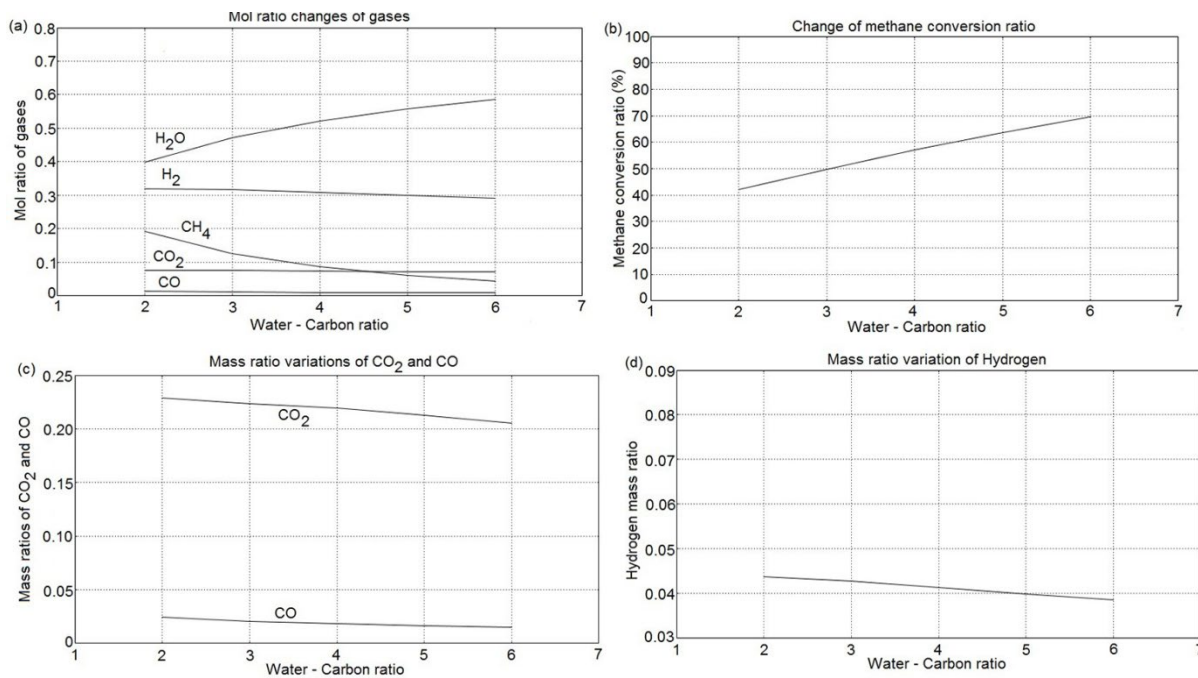


Figure 5 Effects of water/carbon ratios at the inlet of the steam reformer on different system parameters

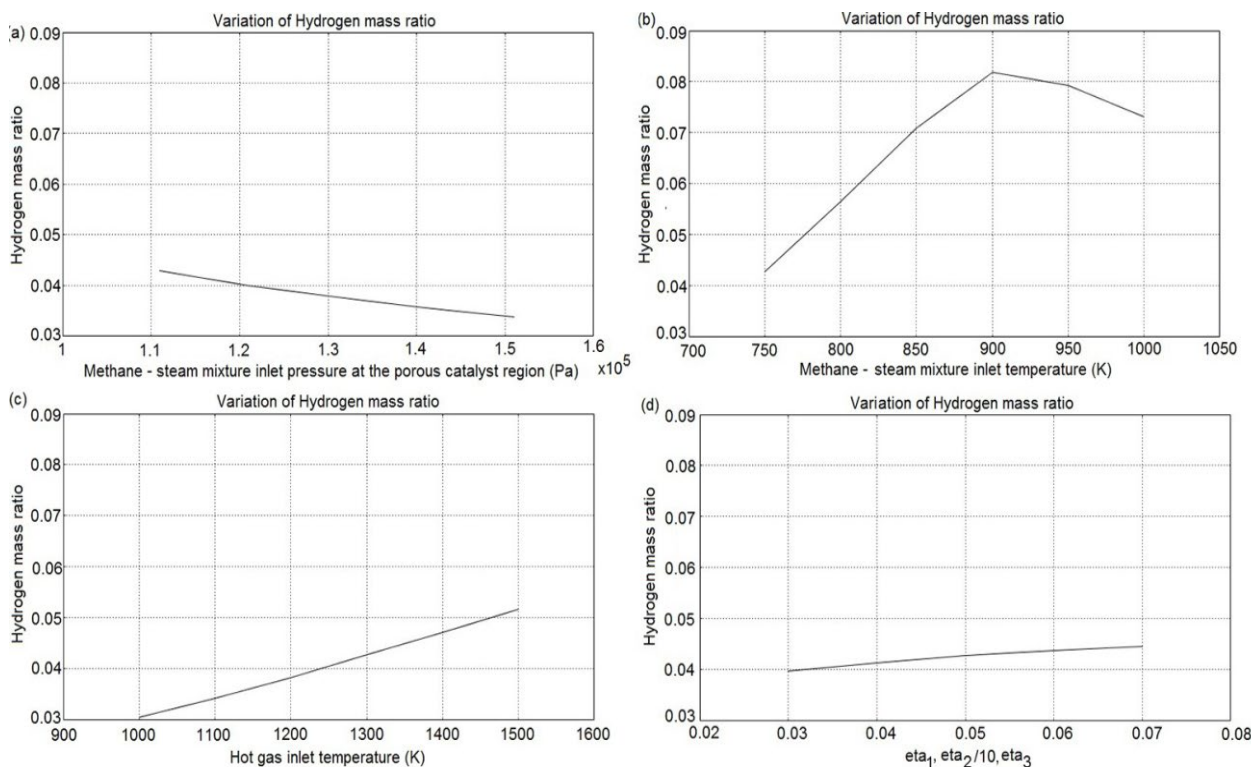


Figure 6 Effects of different system parameters on hydrogen mass ratio in the gas mixture

Figure 7a presents the 2D demonstration of temperature distribution in porous catalyst region. Due to the endothermic reactions occurring in steam reforming process, some gradual temperature changes are seen nearby the steam reformer inlet. Minimum temperature value at this region is 745.938 K. Heat transfer from hot gases at the upper and lower sections to gas mixtures reacting with each other at the porous catalyst section increases the temperature of the hot

gases. As seen, steam reformer inlet temperature of the gas mixture is 750.0 K and its corresponding maximum temperature at the outlet is 785.748 K. Figure 4b shows two dimensional temperature distribution of the hot gas mixture flowing through heating channels taking part at the lower and upper sections of the steam reformer. Inlet temperature of the hot gases is 1300 K. Heat transfer to gas mixture taking place in the steam reforming reactions at the porous catalyst region

causes a considerable decline in temperatures of the gases in the heating channels. Minimum temperature of the gases at the outlet of these channels is 823.443 K. Two dimensional methane mass fraction variation occurred under the effect of steam reforming chemical reactions is shown in Figure 8a. While methane mass fraction value at the inlet is 0.228, outlet methane mass fraction descends to 0.136. As observed from Figure 8a, the amount of steam reforming at inlet section is much more due to high temperature differences between hot gases and methane/steam mixture. Conversion rate decreases moving through the outlet of the steam reformer. Figure 8b visualizes the two dimensional representation of the variation of the steam mass fraction during the steam reforming chemical reactions in the steam reformer. Mass fraction of the steam at the inlet section is

0.769 while minimum value of this parameter at the outlet of the steam reformer is 0.577. Figure 8c depicts the two dimensional plot of the change in hydrogen mass fraction values during the ongoing steam reforming chemical reactions. Endothermic steam reforming reactions maintain the sustainability of the hydrogen production. As a result of this, maximum value of the hydrogen mass fraction at the outlet of steam reformer becomes 0.0428 while hydrogen mass fraction is 0.001 at the inlet section. Due to the significant temperature differences between hot gases and methane /steam mixture at the inlet section, heat transfer is enhanced to some degree and this leads to increase in the amount of steam reforming at the inlet section. Hydrogen production rate decreases as proceeding through channels.

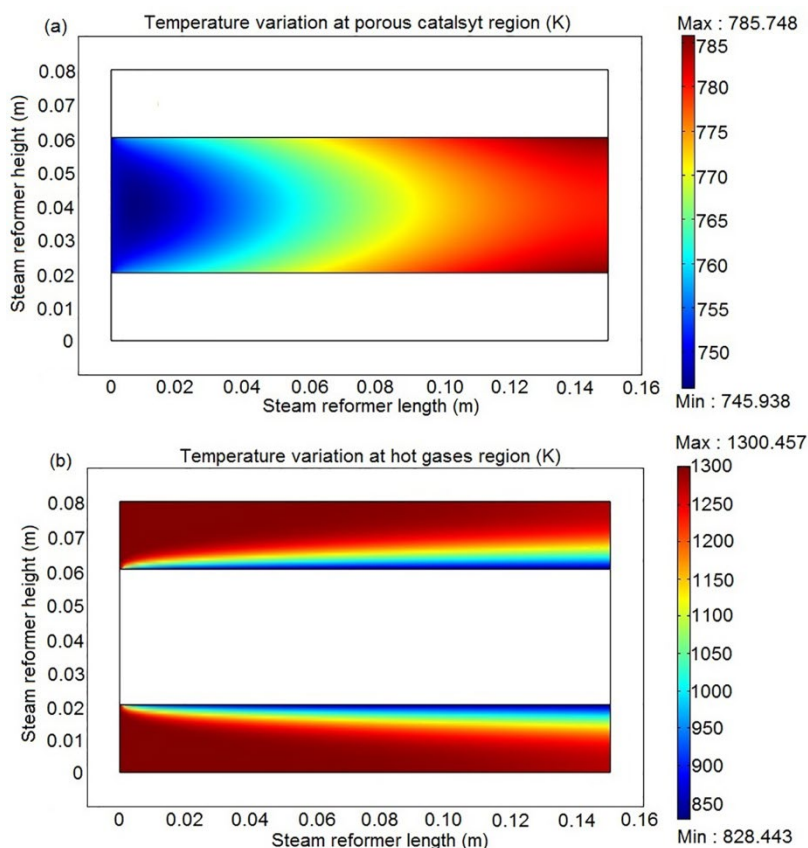


Figure 7 Two dimensional temperature distribution of the gases in the steam reformer

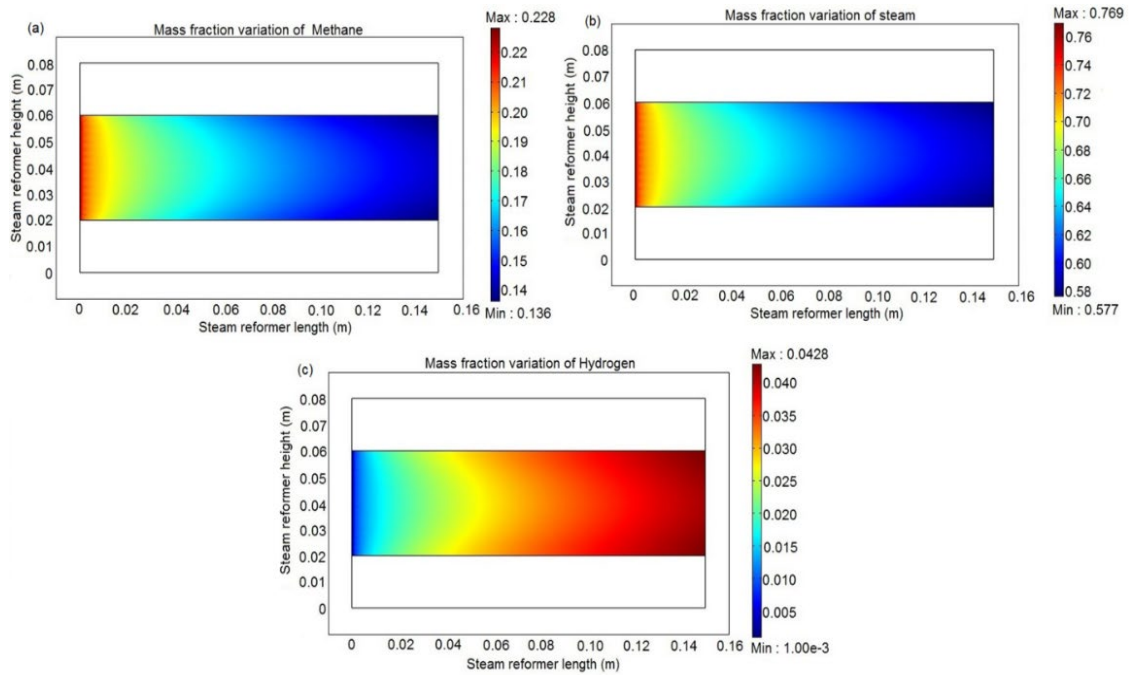


Figure 8 Variational changes of the steam, methane, and hydrogen rates in the steam reformer

9. Conclusion

This study provides a mathematical model for a heat exchanger type small scale isothermal steam reformer. It is considered that the amount of heat supply that is required for endothermic reactions occurred in steam reformer is obtained from the hot gas mixture leaving from the fuel cell. Thus, these gases are allowed to pass through the one side of the heat exchanger. On the other side of the heat exchanger, it is designed to occupy a porous catalyst region across which a steam/methane gas mixture is passing through. Influences of variational model parameters over the amount of produced hydrogen at the steam reformer outlet is investigated based on the developed mathematical model simulated in COMSOL Multiphysics environment. Investigations over the numerical results obtained from this study could pave the way for further researches on catalyst geometry and its influences on total system performance. Heat transfer coefficient between hot gases and catalyst could be attained with considering the dual effects of catalyst geometry and the placement of catalyst in the steam reformer. Furthermore, variations of activity ratios for different catalyst types could be observed by taking into account of variations of the activity ratios of steam reforming reactions across the steam reformer. As temperatures of the hot gases supplied to steam reformer are literally hot waste gases leaving from the fuel cell, intrinsic relationship between steam reformer and fuel cell in terms of working temperatures could be thoroughly investigated. In addition, operational conditions of the steam reformers with varying structural designs could be examined by means of the developed numerical model.

Nomenclature

C_p	Specific heat (J/kgK)
D	Diffusion coefficient (m^2/s)
D_{ij}	Dual diffusion coefficient (m^2/s)
h	Convective heat transfer coefficient (W/m^2K)
ΔH	Enthalpy of reaction (kJ/mol)
k	Heat conductivity (W/mK)
k	Rate coefficient of reaction ($mol.Pa^{0.5}/kg_{cat}$)
K	Equilibrium constant of reaction (Pa^2)
K	Adsorption constant (Pa^{-1})
m_c	Catalyst density (kg_{cat}/m^3)
M	Molar mass (kg/kmol)
n	Total number of gas in the mixture (-)
P	Pressure (Pa)
P_c	Critical pressure (Pa)
P_i	Partial pressure (Pa)
q	Heat flux (W/m^2)
r	Reaction rate ($mol/kg_{cat}.s$)
R	Consumption rate of the reaction ($mol/m^3.s$)
T	Temperature (K)
T_c	Critical temperature (K)
T_r	Reduced temperature (-)
V_c	Critical volume (cm^3/mol)
y	Mol ratio (-)
y_{mi}	Mass fraction (-)
Γ	Heat conductivity resistance (mK / W)
η	Activity coefficients for steam reforming reactions (-)

η	Dipol moment (debye)
κ	Permeability of the porous media (m^2)
μ	Viscosity (Pa.s)
$(\sum v)$	Sum of atomic diffusion volume (cm^3)
ω	Eccentricity factor (-)
Ω_v	Viscosity collosion integral (-)

References

- [1] Erdener H, Erkan S, Erođlu E, Gür N, Şengül E, Baç N, 2007. Sürdürülebilir Enerji ve Hidrojen, ODTÜ Yayıncılık, Ankara, p.105 (in Turkish)
- [2] Siddle A, Pointon KD, Judd RW, 2003. Jones SL, Fuel Processing for Fuel Cells – Status Review and Assessment of Prospects, A report of Advantica Ltd, ETSU F/03/00252/REP. URN 031644 p.124
- [3] Froment GF, Bischoff KB, 2010. Chemical Reactor Analysis and Design, John Wiley and Sons, Canada, p664
- [4] [Ding Y, Alpay E, 2000. Adsorption-enhanced steam methane reforming. Chem Eng. Sci. 55:3929- 3940
- [5] Zamaniyan A, Zoghi AT, Ebrahimi H, 2008. Software development for design and simulation of terraced wall and top fired primary steam reformers. Comput. Chem. Eng. 32:1433-1446
- [6] Zanfır M, Gavriilidis A, 2003. Catalytic combustion assisted methane steam reforming in a catalytic plate reactor. Chem. Eng. Sci. 58: 3947- 3960
- [7] Wilke CH, 1950. A viscosity equation for gas mixtures. J. Chem. Phys. 18: 517- 519
- [8] Chung TH, Lee LL, Starling KE, 1984. Applications of kinetic gas theories and multiparameter correlation for prediction of dilute gas viscosity and thermal conductivity. Ind. Eng. Chem. Fund. 23: 8-13
- [9] Chung TH, Ajlan M, Lee LL, Starling KE, 1988. Generalized multiparameter correlation for nonpolar and polar fluid transport properties, Ind. Eng. Chem. Res. 27: 671- 679
- [10] Poling BE, Prausnitz JM, O’Connell JP, 2007. The Properties of Gases and Liquids, McGraw Hill, Singapore, p.768
- [11] Wassiljewa A, 1904. Heat conduction in gas mixtures. Physik. Z. 5: 737 – 742
- [12] Mason EA, Saxena SC, 1958. Approximate formulae for the thermal conductivity of gas mixtures. Phys. Fluid 1: 361 – 369
- [13] Yaws CL, 1999. Chemical Properties Handbook, McGraw Hill, New York, p780
- [14] Blanc, MA, 1908. Recherches sur les mobilites des ions dans les gaz. J. Phys. 7: 825 – 839
- [15] Fuller EN, Giddings JC, 1965. A comparison of methods for predicting gaseous diffusion coefficients. J. Chromatogr. Sci. 3: 222- 227
- [16] Fuller EN, Schettler PD, Giddings JC, 1966. New method for prediction of binary gas-phase diffusion coefficients. Ind. Eng. Chem. 58: 18- 27
- [17] Fuller EN, Ensley K, Giddings JC, 1969. Diffusion of halogenated hydrocarbons in helium. The effect of structure on collision cross sections. J. Phys. Hem. 73: 3679-3685
- [18] Hoang, D.L., Chan, S.H., and Ding, O.I., 2005, Kinetic and modelling study of methane steam reforming over sulfide nickel catalyst on a gamma alumina support, Chemical Engineering Journal, 112:1–11.